Multi-material 3D Printing of Thermoplastic Elastomers for Development of Soft Robotic Structures with Integrated Sensor Elements

Antonia Georgopoulou[1,2(✉)], Bram Vanderborght[2],
and Frank Clemens[1]

[1] Department of Functional Materials,
Empa – Swiss Federal Laboratories for Materials Science and Technology,
Überlandstrasse 129, 8600 Dübendorf, Switzerland
antonia.georgopoulou@empa.ch
[2] Department of Mechanical Engineering (MECH), Vrije Universiteit Brussel
(VUB), and Flanders Make, Pleinlaan 2, 1050 Brussels, Belgium

Abstract. Embedded sensing can benefit soft robots with the ability to interact with their environment but producing embedded soft sensors can be challenging. Multi-material Fused Deposition Modeling (FDM) additive manufacturing allows producing complex structures, by combining more than one kind of polymeric material. For multi-material FDM, conductive thermoplastic elastomer filaments have been developed. This allows the printing of flexible functional structures, based on thermoplastic elastomer structures with conductive paths that are of great interest for stretchable electronics and soft robotic applications. In this study, stretchable piezoresistive elastomer strain sensor composites were successfully produced by using multi-material FDM. A piezoresistive thermoplastic elastomer was printed on the top of a nonconductive, flexible thermoplastic elastomer strip using FDM multi-material 3D printer. FDM elastomer filaments with different shore hardness as substrate materials for the gripper structure were used. The hardness of the elastomer affected the printability and the adhesion to the conductive elastomer material, which was used as a strain sensor material. The hardness affected the strain sensor properties too. The piezoresistive response, dynamic behavior, drift, relaxation and sensitivity of the printed multi-material strips were investigated by tensile tests. Soft robotic grippers with integrated sensing elements to detect deformation while touching the objective were selected as a case study. The soft grippers with the integrated sensors exhibited intelligent response by recognizing when they were griping a small or big object and when an obstacle was inhibiting their function.

Keywords: Piezoresistive elastomer sensor · FDM additive manufacturing · Soft robotic gripper

1 Introduction

Important applications for additive manufacturing (AM) are the development and fabrication of products for consumer goods and electronics [1]. 3D printing in combination with functional materials can be used for the production of sensors integrated in substrates and robotic devices [2–4]. The FDM additive manufacturing is one of several material extrusion methods, which can be used to develop robotic devices with integrated sensors. One of its main advantages in comparison to direct energy deposition, material jetting or powder bed fusion AM techniques is the fact that multi-material printing is easy to implement. In addition, FDM is cost-efficient, has good resolution and compatibility with many materials and composites [5, 6]. Multi-mateiral FDM includes a combination of different materials and can be a useful production method for robotic systems [7]. In the case of sensing in robotics, multi-material 3D printing can be used for producing the robotic body with integrated sensors, based on functional materials, in one-step [8]. FDM additive manufacturing is compatible with thermoplastic elastomer materials like thermoplastic polyurethane (TPU). By using TPU filaments, it is possible to print soft robotic structures like pneumatic actuators and grippers.

Soft robotic grippers with integrated sensors are intelligent systems that can alter the posture, gripping force, and gripping geometry according to the object they are gripping [9, 10]. These intelligent grippers can find application where a careful manipulation of objects is needed but also for the handling of complex geometries, where compliance with the object surface is important [11]. Therefore, soft grippers have been developed for the food industry to handle sensitive food and perform complex tasks that involve food like packaging [12, 13]. Furthermore, the soft robotic gripper can be used for the exploration of unknown environments like space or underwater and can be particularly useful for acquiring sensitive samples from these environments [14, 15]. Soft grippers based on pneumatic actuators can be controlled by pressure [16]. It is also possible to develop soft grippers using servomotors. However, they must be controlled optically or by piezoresistive sensors to be able to use them for sensitive objectives. Under harsh conditions, optically monitoring of gripper movements is difficult. Multi-material FDM to develop soft robotic grippers with integrated sensors has been used before [17]. However, the effect of the stiffness of the soft gripper structure on the sensing behavior has never been investigated. In this attempt, soft robotic grippers with integrated strain sensors have been investigated using a commercial FDM multi-material printer. TPU filament with carbon black filler was used for printing of the sensing paths on the surface of the gripper structure. The body of the soft gripper was printed with TPU filaments of two different shore hardness to investigate the effect of the shore hardness on the sensing behavior of the conductive sensing structure on the surface of the gripper. Furthermore, the effect of the thickness of the gripper on the sensing behavior was investigated and the potential of the sensor to be used for monitoring the function of the robotic gripper was explored.

2   Materials and Methods

2.1   Sensor Printing and Robotic Gripper

Filaments based on TPU were supplied from Recreus Industries (Elda, Spain) in two different shore harnesses (FilaFlex 82A and FilaFlex 95A). The conductive TPU filament Eel based on thermoplastic polyurethane and carbon black was supplied by Fenner Drives (Ninjatek Eel, Manheim, USA). For 3D printing, the FDM 3D printer Pro2 Dual Extruder 3D Printer (Raise 3D, Irvine, USA) was used. The printing of the multi-material strips and soft grippers was done at a temperature of 230 °C with a printing speed of 15 mm/s for the perimeters and 20 mm/s for the infill. A layer height with 0.2 mm was printed with a nozzle size of 0.6 mm. To achieve a dense structure, infill was set to 100%; the extrusion multiplier was set to 120%. The setup of the multi-material FDM additive manufacturing process can be seen in Fig. 1.
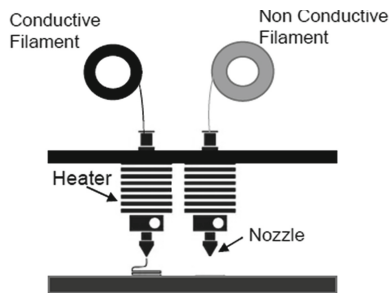

Fig. 1. Setup of the process of multi-material FDM additive manufacturing with a conductive and a non-conductive filament.

For the assessment of the mechanical and electrical behavior of the system, the Eel conductive TPU was printed on the surface of TPU strips with dimensions 130 × 10 × 0.3 mm.

For the multi-material soft gripper structure, first, the sensor structure was produced and on top of it, the gripper body was printed. After the printing of the gripper, silver wires were inserted at the gripper to act as tendons. These tendons were necessary for the actuation and motion of the robotic gripper. Additional to the wires, a Tower Pro MG90S micro servo (Adafruit Industries. New York, USA) was used. The control of the motor was performed with an Arduino microcontroller. Both structures are shown in Fig. 2.
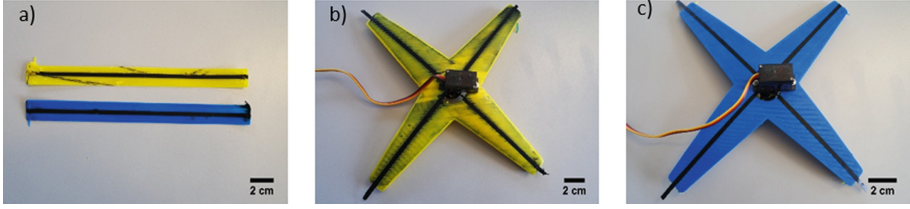
Fig. 2. a) Sensors integrated on the surface of an elastomer strip from FilaFlex 82A (yellow) and FilaFlex 95A (blue) b) robotic gripper with integrated sensing elements made with FilaFlex 82 and c) with FilaFlex 95A for the robotic body using multi-material 3D printing.

2.2 Tensile Testing

For minimizing the slipping during the tensile testing, pneumatic clamps were used. 4 bar pressure had to be applied to avoid slipping of the samples during the testing. For measuring the resistivity during the tensile test, a Keithley 2450 source meter (Keithley, Solon, USA) was used with the KickStart software from the same company. For the measurements, a two-terminal sensing mode was used and the change in current was measured while a constant voltage of 1 V was applied. Two different types of tensile tests were performed. First, the strips were tested up to the breaking point, and later strips were tested dynamically with consecutive cycles of loading and releasing, separated by a dwell time of 30 s at the maximum and minimum strain levels. From the measurements of the resistance, the relative resistance (R_{rel}) was calculated according to the formula where R is the electrical resistance of the sensor and Ro the electrical resistance of the sensor when no strain is applied to it:

$$R_{rel} = \frac{R - R_0}{R_0} \tag{1}$$

3 Results and Discussion

3.1 Tensile Test to the Breakpoint

Tensile tests were performed on multi-material printed strips (Fig. 2a). From the results of the tensile test, the stress-strain was constructed (Fig. 3).
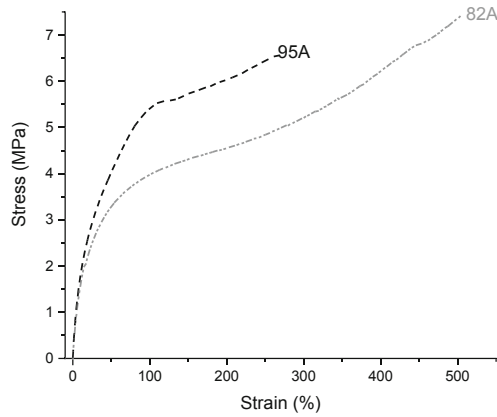
Fig. 3. Stress-strain plot of the TPU strips (with integrated sensor element) with different shore hardness (82A and 95A). The strip with the lowest shore hardness could endure larger elongations compared to the substrate of higher shore hardness.

From the stress-strain plot, it can be seen, that the TPU with lower shore hardness could endure much larger elongation (up to 500%) before the break. The strip with higher shore hardness broke at 260% strain. As expected, the stiffness was higher for the strip, which was printed from TPU filament with higher shore hardness. The elasticity modulus was calculated at 13 MPa for the 82A strip sample and 23 MPa for the 95A sample. No delamination between the sensor part and the substrate strip was observed during the tensile testing. The sensor broke before the substrate strip did.
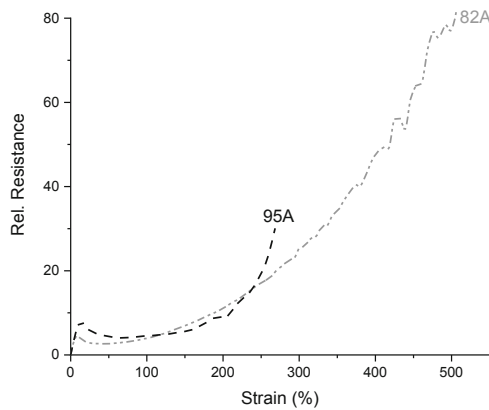

Fig. 4. Electrical signal of the piezoresistive sensor printed on the TPU strips of different shore hardness.

Looking at the sensor response (Fig. 4), up to 250% strain, the strips of the two different TPU strips show similar behavior. The electrical resistance changed with the applied deformation, showing that the system exhibited a piezoresistive response.

3.2   Dynamic Tensile Testing

Looking at the dynamic testing (Fig. 5), it was seen that after five cycles of loading and releasing, the mechanical properties of the strips with integrated sensor elements responded with good repeatability.
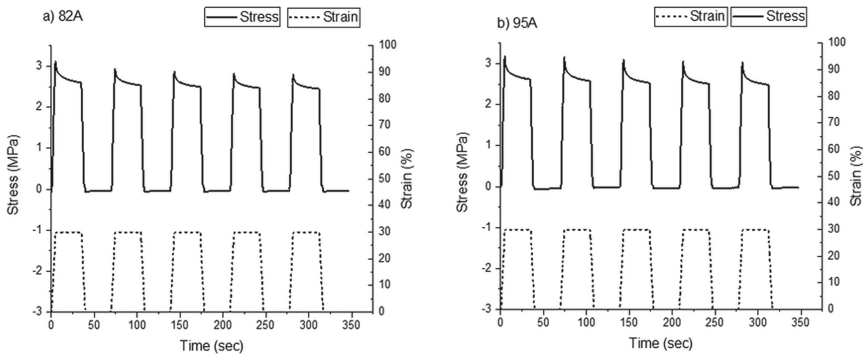

Fig. 5. Mechanical response during dynamic tensile testing between the strain 0 and 30% for strips of shore hardness a) 82A and b) 95A. Stress relaxation was observed for both sensor systems but was larger for the strip of lower shore hardness.

At the dwell time, when the strain was held constant for 30 s the mechanical relaxation was investigated as described by Melnykowycz et al. [18]. Stress relaxation often occurs in elastomers and can affect the sensor response during the dynamic test. As proposed by Melnykowycz et al., the drift of the mechanical stress was investigated between different cycles. In this case, the drift between the second and fifth cycle at 30% strain was evaluated (Table 1).

Table 1. Mechanical relaxation and drift during dynamic tensile testing for strips made with multi-material 3D printing calculated at 30% strain.

Substrate material	Mechanical relaxation	Mechanical drift
FilaFlex 82A	24%	20%
FilaFlex 95A	20%	5%

It was observed that at 0% strain, the strips were bucking and therefore the mechanical relaxation and drift could not be calculated. Based on the measurements shown in Fig. 4, buckling occurred at strains below 16%. The stress relaxation was higher in the case of the material with the lower shore hardness, FilaFlex 82A. As for

the mechanical drift, it was relatively low for both systems, except for the FilaFlex 95A system with a drift of 89%. The presence of drift especially at low strains can be attributed to the presence of buckling during the tensile testing.

Looking at the piezoresistive behavior of the 3D printed sensor elements on top of the TPU strips during the dynamic testing it was seen, that the relative resistance could follow the change in strain for both the loading and the releasing phase of the tensile test (Fig. 6).
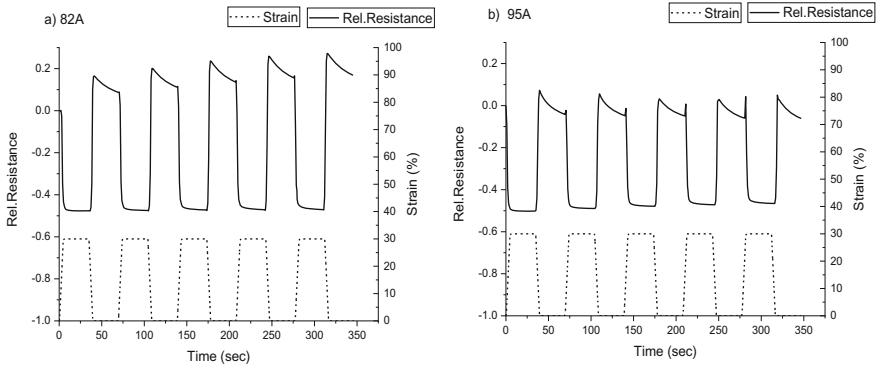

Fig. 6. Sensor Response during dynamic tensile testing between the strain 0 and 30% for embedded sensors in substrates with shore hardness a) 82A and b) 95A. Relaxation was also observed for the electrical signal but in this case, there was not significant dependence on the shore hardness of the strip observed.

The reverse piezoresistivity that was seen during the tensile test to the breakpoint for strains lower than 30%, was also seen at the dynamic testing. At low strain higher conductivity and at high strain lower conductivity can be observed. It is worthwhile to mention that due to the buckling behavior, the electrical relaxation and drift could not be determined at 0% strain. However, it can be seen in Fig. 6, that during buckling of the strips at lower than 16% strain the electrical signal of the 82A show an unexpected drift. The response of the sensor was linear but the relative resistance decreased with an increase in strain and increased when the strain decreased. The relaxation and drift that was observed for the mechanical dynamic behavior of the sensor, was also seen in the response of the sensor signal (Table 2).

Table 2. Electrical relaxation and relaxation during dynamic tensile testing for the sensors integrated into an elastomer substrate produced with multi-material 3D printing calculated at 30% strain.

Substrate material	Electrical relaxation	Electrical drift
FilaFlex 82A	28%	9%
FilaFlex 95A	25%	8%

In the case of the electrical signal, the relaxation was slightly higher for the system with a strip of lower shore hardness. This finding agreed with what was also observed for stress relaxation. However, in the case of the drift of the electrical signal, there was almost no difference seen when comparing the two systems.

3.3   Application: Robotic Gripper with Integrated Piezoresistive Gauge Sensor

The aim of this study was the printing of soft robotic grippers with integrated strain sensing elements. The grippers consisted of a flexible belt and elements called phalanges (Fig. 7).
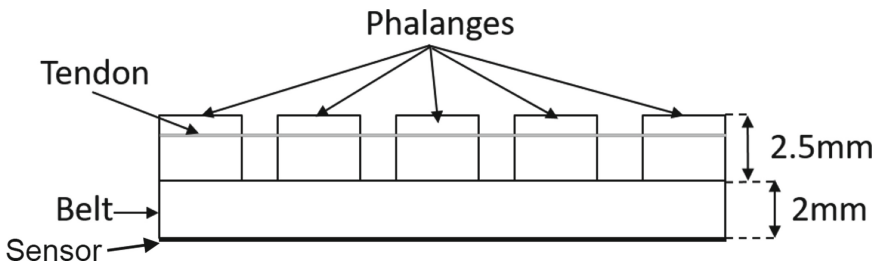

Fig. 7. Sketch of a tentacle, showing the belt, the phalanges and the wires (tendons) which are connected to the servomotor.

Inside the phalanges structure, a wire (tendon) is connected with a servomotor. If the servomotor will coil the tendon, the belt will bended until the phalanges will touch each other. With the assistance of flexible tendons, the belt could bend because of the reduction in tendon length that is connected to the servomotor. The black lines in Fig. 7 are the piezoresistive sensor parts, which were printed on top of the belt structure. Varying thickness of the belt from 2 to 6 mm was used to investigate the effect of the geometrical stiffness, and therefore the bending stress and deformation, on the sensor behavior. Grippers with three different belt thicknesses (2 mm, 4 mm and 6 mm) were printed. The grippers were assessed for their sensor performance during consecutive cycles of opening and closing (Fig. 8).
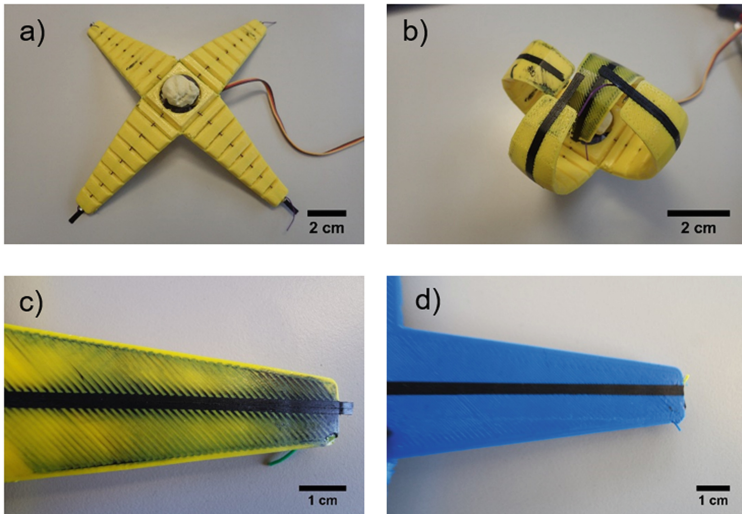
Fig. 8. Gripper with embedded sensors produced with multi-material FDM additive manufacturing operates between positions a) open and b) closed and close up for the gripper of shore hardness c) 82A and d) 95A.

It is worthwhile to mention that by adding the sensor structure on top of the printed gripper substrate no significant stiffening effect could be observed and the servomotor had no problem opening and closing the gripper. Based on mechanics for bending, the sensor will see larger stress and deformation if the thickness of the gripper will increase. As it was seen from the sensor response, by increasing the belt thickness, the change in the electrical resistance of the strain sensor decreased (Fig. 9).
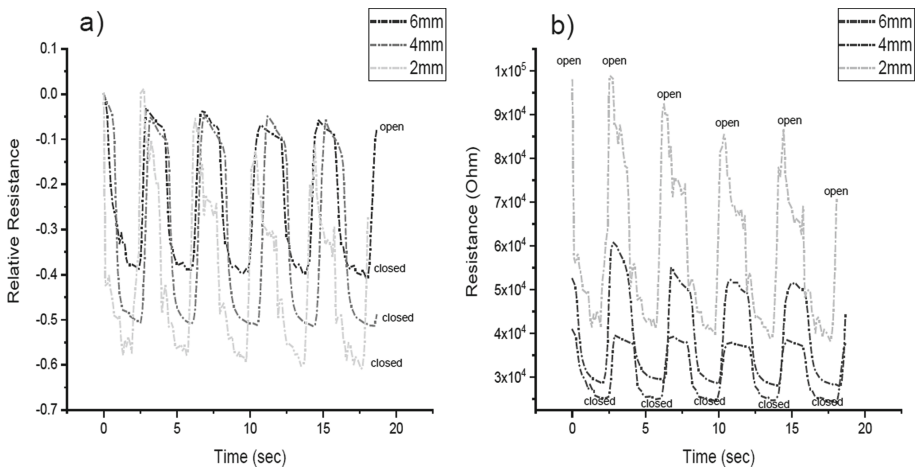

Fig. 9. Signal response of the strain sensor on the surface of the belt structure in a robotic gripper with three different belt thicknesses during a cyclical test. The gripper moved five times between positions open and close a) relative resistance during testing and b) resistance during the testing. The gripper with a belt of the smallest thickness had the largest change in relative resistance but the sensor response was accompanied by significant noise.

Independent on the belt thickness, all the grippers showed the reverse piezoresistivity that was seen during the tensile testing (Fig. 6). In general, for all belt thicknesses it could be observed that while the deformation increased, the relative resistance decreased. For the gripper with the smallest thickness of the belt, it was seen that the change in the resistance and relative resistance was the highest. However, when looking at the gripper with the 2 mm belt thickness, observed higher noise at a closed position and a lager relaxation at an open position can be observed. The appearance of this noise could be considered undesirable for many applications like soft robotics and might be an artifact of the servomotor because of small voltage fluctuations. This noise was only observed in the gripper with the smaller belt thickness and is not noticeable for the other systems. The relative resistance change changes for the three different grippers. To verify these differences, some deformations calculations where done (Table 3).

Table 3. The deformation of the gripper and change in relative resistance when the gripper moved between positions open and close for grippers with different belt sizes.

Belt thickness (mm)	Length of the wire at open position (mm)	Length of the wire at close position (mm)	Relative deformation	Relative change in resistance
2	8	9.8	20.2%	60%
4	8	9.2	14.0%	52%
6	8	8.8	9.5%	37%

The wires were used to open and close the tentacles of the soft grippers by a servomotor and the change in their length, when the gripper moved between positions open and closed, was used to calculate the relative deformation. The wires were coiled up and thus the length of the wires gets shorter when the gripper is closed. Looking at the values in Table 3 it was observed, that the relative deformation decreased by increasing the belt thickness. Smaller deformation caused a smaller change in resistance, an effect that is expected from a deformation sensor. The results in Table 3 are in good agreement with optical observations. Due to the design change of the gripper (thicker band) it was observed, that the phalanges would touch each other at lower strain, which will block further deformation of the tentacle of the gripper.

The initial value Ro for the resistance was also different for the grippers with different band thicknesses (Fig. 9b). The Ro was higher for the gripper with the lowest belt thickness and decreased with the increasing belt thickness. In order to verify if this difference was caused by the printing procedure, the initial resistance Ro was measured for all the four tentacles of each gripper (Table 4).

Table 4. The deformation of the gripper and change in relative resistance when the gripper moved between positions open and close for grippers with different belt sizes.

Gripper material	Belt thickness (mm)	Ro at tentacle 1 (kΩ)	Ro at tentacle 2 (kΩ)	Ro at tentacle 3 (kΩ)	Ro at tentacle 4 (kΩ)	Deviation
FilaFlex 82A	2	36 ± 6	34 ± 8	79 ± 2	102 ± 6	29%
FilaFlex 82A	4	164 ± 4	120 ± 5	48 ± 1	33 ± 3	53%
FilaFlex 95A	4	59 ± 4	67 ± 5	60 ± 4	58 ± 3	4%
FilaFlex 82A	6	116 ± 3	50 ± 1	31 ± 2	33 ± 2	35%

From comparing the values of the resistance in the different tentacles, it was seen that the values can vary a lot for all the grippers made with the material FilaFlex 82A. The change in resistance was the same for every tentacle, independent of the initial value in the resistance as it is a parameter that depends on the deformation, which was the same for all the tentacles. As a result, there can't be made a conclusion about the effect of the thickness of the belt on the values of the resistance. However, this was not the case for the material FilaFlex 95A. In this system, the values of the resistance had consistency between the different tentacles of the grippe. This large deviation in the values of the resistance can be traced back to the printing procedure. When observing optically the produced grippers, for the case of FilaFlex 82A material that there could be seen traces of carbon black powder all over the first layer. This effect was distinguished as the original color of the filament appeared darkened by black particles at parts of the first layer. This was not the case for the FilaFlex 95A gripper, that the coloration of the first layer was unaltered. A possible interpretation is that during the printing, in the case of the FilaFlex 82A, the nozzle that printed the robotic body carried away some of the particles of the carbon black of the conductive TPU that was print first. However, this change was not consistent during the printing, the discoloration appeared more intense in some tentacles compared to others, and this could be an explanation for the deviation of the values of the resistance.

Based on those results of the gripper design study, grippers with a belt thickness of 4 mm were made with the FilaFlex 82A the FilaFlex 95A. The grippers were compared for the electrical signal and stability of the sensor response. Both structures showed a relative deformation of around 16% for a fully closed position. In order to assess the sensor signal for the grippers, the soft structures were opened and closed with a dell time during each position. In addition, an objective (orange) was grabbed by the soft grippers (Fig. 10 a)). In addition, the electrical signal of the sensor was investigated when the movement of the tentacles was blocked by an obstacle (Fig. 10 b)).
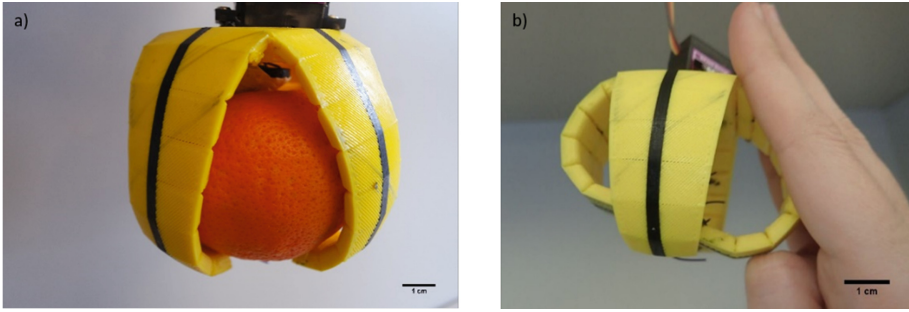
Fig. 10. a) The robotic gripper with the integrated sensors and a band thickness of 2 mm is gripping an orange to test object recognition and b) the hand is preventing the gripper from opening to test obstacle recognition by the integrated sensor.

The sensor response for the grippers made with the materials of different shore hardness performing different tasks can be seen in Fig. 11
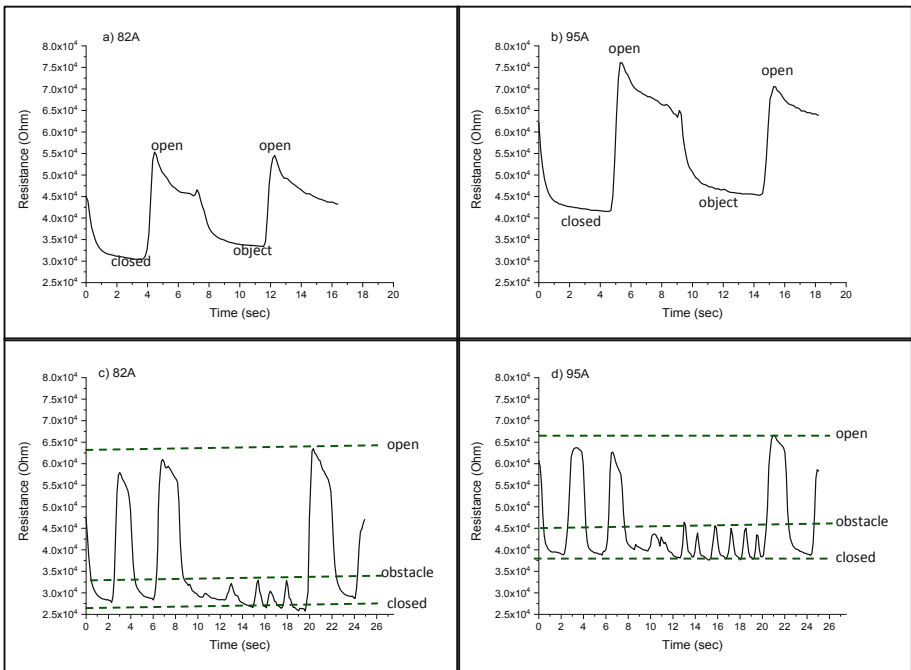

Fig. 11. Sensor response for grabbing objective and obstacle during obstacle recognition test for grippers with a robotic made out of elastomer with shore hardness a) 82A and b) 95A and sensor response during obstacle recognition test for the robotic body made out of elastomer with shore hardness c) 82A and d) 95A. Both sensors could indicate when the gripper was gripping an object, when not and when an obstacle was impairing the function of the system

Looking at Fig. 11 a) and b) it was calculated, that the difference in resistance was 52% for the 82A and 59% for the 95A. The relative change in resistance between the closed positions and holding an objective was 7.4% and 11.5% for the 82A and 95A, respectively. Therefore, in both cases, the relative change of the sensor signal was slightly higher for the TPU gripper with higher shore hardness. An important parameter for deformation sensors that are targeted for robotic applications is the ability to distinguish from the sensor signal the different positions of the robot system. The initial resistance at 6.1 kΩ was higher for the system with higher shore hardness compared to the lower shore hardness, with initial resistance of 4.2 kΩ.

As already mentioned, the maximal deformation from open to the closed position (touching of the phalanges) was 16.2%. For grabbing the orange, the deformation was calculated to 6.5%. According to the electrical resistance values, the piezoresistive sensors integrated into the soft gripper structures can identify if the gripper is open, closed or if an objective is grabbed. In soft robotics, grippers with integrated piezoresistive sensor elements that can distinguish between when the gripper is grabbing an object, open and closed position lead to the creation of intelligent robotic systems.

Additionally to the gripping test, an obstacle test was performed. During the obstacle test, the gripper movement (open-closed-open-closed) was blocked manually after two cycles. In the first two, the closing and opening of the soft gripper could be easily detected by the change in resistance. However, at the time point when the obstacle was imposed, the value for the resistance did not return to the value of the resistance for the open position. As already explained, wires were used to open and close the tentacles of the soft grippers by a servomotor. The wires are coiled up and thus the length of the wires gets shorter when the gripper is closed. The resistance stayed close to the value for the closed position for the entire time the obstacle was imposed. After the obstacle was removed, the resistance returned to the previous values for the position open.

With the ability to distinguish between positions open and close, but also recognizing obstacles and when the gripper is gripping an object, these intelligent soft robots can be used for applications where effective monitoring of the gripper function is needed. As a result, these grippers with integrated sensing elements could be used for more efficient production in many sectors of the industry that requires soft robots, as it is, for example, the food industry.

In this attempt, soft robotic grippers with integrated sensing elements were produced in the one-step process using multi-material FDM. These grippers consisted of two materials, one conductive TPU that can be used to sense the deformation of the gripper structure and one non-conductive TPU to fabricate the structure of the gripper. In order to investigate, the behavior of the printed composite systems and the effect of the shore hardness of the strips, tensile testing was performed. The TPU with lower shore hardness can be used for applications with larger elongation. However, cycling experiments showed that the sensor behavior was similar for both types of TPU.

4   Conclusions

For the functional soft gripper application, first, the optimal thickness of the sensor part of the soft gripper was adjusted to 4 mm thickness. Later, two TPU filaments with different shore hardness (82A and 95A) were investigated as candidate materials for the gripper structure. The gripper with the TPU 95A showed a slightly higher difference in electrical resistance value between open and closed positions. This resulted in a higher sensitivity. The grippers with the integrated sensing elements exhibited intelligent function. The deformation of the sensor enriched their function with the ability to distinguish when the gripper is gripping an object, when not and when an obstacle is preventing the gripper from functioning properly. This intelligent soft robotic gripper with the integrated sensors that was produced in one-stem with a simple and low cost could be potentially found each place in production lines for sensitive objects and lead to more efficiency and accuracy in production.

References

1. Ligon, S.C., Liska, R., Stampfl, J., Gurr, M., Mülhaupt, R.: Polymers for 3D printing and customized additive manufacturing. Chem. Rev. **117**, 10212–10290 (2017)
2. Yang, Y., Song, X., Li, X., Chen, Z., Zhou, C., Zhou, Q., Chen, Y.: Recent progress in biomimetic additive manufacturing technology: from materials to functional structures. Adv. Mater. **30**, 1706539 (2018)
3. Yap, H.K., Ng, H.Y., Yeow, C.H.: High-force soft printable pneumatics for soft robotic applications. Soft Robot. **3**, 144–158 (2016)
4. Mutlu, R., Alici, G., Panhuis, M.I.H., Spinks, G.M.: 3D printed flexure hinges for soft monolithic prosthetic fingers. Soft Robot. **3**, 120–133 (2016)
5. Mohan, N., Senthil, P., Vinodh, S., Jayanth, N.: A review on composite materials and process parameters optimisation for the fused deposition modelling process. Virtual Phys. Prototyp. **12**, 47–59 (2017)
6. Kumar, S., Kruth, J.P.: Composites by rapid prototyping technology. Mater. Des. **31**, 850–856 (2010)
7. Espalin, D., Muse, D.W., MacDonald, E., Wicker, R.B.: 3D printing multifunctionality: structures with electronics. Int. J. Adv. Manuf. Technol. **72**, 963–978 (2014)
8. Shih, B., Christianson, C., Gillespie, K., Lee, S., Mayeda, J., Huo, Z., Tolley, M.T.: Design considerations for 3D printed, soft, multimaterial resistive sensors for soft robotics. Front. Robot. AI. **6**, 30 (2019)
9. Zhou, J., Chen, S., Wang, Z.: A soft-robotic gripper with enhanced object adaptation and grasping reliability. IEEE Robot. Autom. Lett. **2**, 2287–2293 (2017)
10. Manti, M., Hassan, T., Passetti, G., D'Elia, N., Laschi, C., Cianchetti, M.: A bioinspired soft robotic gripper for adaptable and effective grasping. Soft Robot. **2**, 107–116 (2015)
11. Shintake, J., Cacucciolo, V., Floreano, D., Shea, H.: Soft robotic grippers. Adv. Mater. **30**, 1707035 (2018)
12. Wang, Z., Torigoe, Y., Hirai, S.: A prestressed soft gripper: design, modeling, fabrication, and tests for food handling. IEEE Robot. Autom. Lett. **2**, 1909–1916 (2017)

13. Naghdy, F., Esmaili, M.: Soft fruit grading using a robotics gripper. Int. J. Robot. Autom. **11**, 93–101 (1996)
14. Hao, Y., Wang, T., Ren, Z., Gong, Z., Wang, H., Yang, X., Guan, S., Wen, L.: Modeling and experiments of a soft robotic gripper in amphibious environments. Int. J. Adv. Robot. Syst. **14**, 1729881417707148 (2017)
15. Licht, S., Collins, E., Mendes, M.L., Baxter, C.: Stronger at depth: jamming grippers as deep sea sampling tools. Soft Robot. **4**, 305–316 (2017)
16. Yang, Y., Chen, Y.: Innovative design of embedded pressure and position sensors for soft actuators. IEEE Robot. Autom. Lett. **3**, 656–663 (2018)
17. Schmitt, F., Piccin, O., Barbe, L., Bayle, B.: Soft robots manufacturing: a review. Front. Robot. AI. **5**, 84 (2018)
18. Melnykowycz, M., Koll, B., Scharf, D., Clemens, F.: Comparison of piezoresistive monofilament polymer sensors. Sensors **14**, 1278–1294 (2014)